Applying PySCMGroup to Breast Cancer Biomarkers Discovery

Mazid Abiodoun Osseni[1][a], Prudencio Tossou[1,2][b], Jacques Corbeil[1][c] and François Laviolette[1,3][d]

[1]*Université Laval, Québec, Canada*

[2]*InVivo AI, Montréal, Canada*

[3]*Mila, Montréal, Canada*

Keywords: Multi-omics, Breast Cancer, Interpretability, Penalty-weight, Pathway Guided Selection.

Abstract: **Background.** The identification of biomarkers associated with triple-negative breast cancer (TNBC) is still an active area of research due to the complexity of finding robust biomarkers associated with the disease. Previous methods have attempted to tackle the problem from a mono-perspective view by analyzing each omics individually in the search of biomarkers. The majority of these methods mainly focus on gene expression analysis since their impact on the phenotype is easier to measure and possibly more direct. However, it is common understanding that genes belong to pathways and tend to work together within various metabolic, regulatory, and signalling pathways. Hence, in this work, we tackled the TNBC biomarker discovery problem as a multi-omic pathway-based problem by efficiently combining the biological knowledge from multiple pathways using a novel machine learning algorithm. The proposed algorithm, called GroupSCM, is an extension of the Set Covering Machine (SCM) that incorporate the pathway features as priors.

Results. Although the GroupSCM performed similarly to the SCM, metric-wise, it helps identify new biomarkers not previously found by the SCM. By leveraging the pathway priors, the GroupSCM was able to uncover two miRNAs: hsa-mir-18a and hsa-mir-190b, already known to be associated with various cancers including breast cancer and yet to be linked to the Triple-Negative Breast Cancer phenotype.

Conclusion. The addition of priors to the SCM leads to interpretable, complete and sparser models which are easier to analyze *in vivo* settings. It also provides insight into the omics interaction by highlighting the miRNAs and epigenome contribution to the prediction task.

Code Availability: The code is available at: https://github.com/dizam92/BRCA_experiments_and_paper

1 INTRODUCTION

Based on their genes expression, breast cancer (BC) cases can be sub-classified into five categories: luminal A, luminal B, HER2++, Basal like and Triple-Negative Breast Cancer (TNBC) (Lehmann et al., 2011). TNBC, characterized by the non-expression of estrogen (ER), progesterone (PR), and HER2 receptors, represents 10-20% of all breast cancers and is known to be the most aggressive form, i.e. most likely to spread beyond the breast and recur post-treatment (Weigelt et al., 2010). Unfortunately, TNBC still remains poorly diagnosed, as clinical, microarray-based studies and immunohistochemical profiling are often inconclusive, due to its similarity with the basal-like breast cancer type. Consequently, there is a need for the discovery of additional biomarkers to improve the clinical diagnostic and prediction prognosis between TNBC and other breast cancer types.

Genetic studies of cancer diseases in general have often focused on extracting information from association analysis using only a few types of data. For example, (Iorio et al., 2005) showed that, compared with normal breast tissue, miRNAs (specifically miR-125b, miR-145, miR-21 and miR-155) are also aberrantly expressed in human Breast Cancer. In the case of the Colorectal Cancer (CRC), (Lao and Grady, 2011) put more emphasis on the fact that the hyper-methylation of some CpGs site ahead of certain genes (CXCL12) can promote the metastatic behaviour of colon cancer cell lines. However, to better understand the disease's complex genetic explanation and in order to provide robust biomarkers, it is becoming increasingly important to inte-

[a] https://orcid.org/0000-0001-7358-7402
[b] https://orcid.org/0000-0002-9841-9867
[c] https://orcid.org/0000-0002-9973-2740
[d] https://orcid.org/0000-0002-1937-2512

Osseni, M., Tossou, P., Corbeil, J. and Laviolette, F.
Applying PySCMGroup to Breast Cancer Biomarkers Discovery.
DOI: 10.5220/0010375500720082
In *Proceedings of the 14th International Joint Conference on Biomedical Engineering Systems and Technologies (BIOSTEC 2021) - Volume 3: BIOINFORMATICS*, pages 72-82
ISBN: 978-989-758-490-9

grate and utilize the full scope of available omics information, recorded from a wide range of experimental modalities (Freedman et al., 2011), (Karczewski and Snyder, 2018). Embracing this philosophy, numerous studies combined omics to tackle the biomarkers discovery problem. Using unbiased multi-omics approaches, (Yuan et al., 2016) reported that DNA topoisomerase 2 beta (TOP2B) shows a male-biased difference in DNA methylation in Bladder Cancer. In the case of Calcific Aortic Valve Disease (CAVD), (Heuschkel et al., 2020) demonstrated that the multi-omics integration of overlapping proteome/transcriptome molecules, with the miRNAs, identified a CAVD protein–protein interaction network. Meanwhile (Rappoport et al., 2020) introduced MONET (Multi Omic clustering by Non-Exhaustive Types) aimed at discovering modules of similar samples such that each module is allowed to have a clustering structure for only a subset of the omics. This is a multi-omics clustering approach which differs from the other algorithms by not assuming a common structure across all omics data. (Delogu et al., 2020) proposed that upgrading multi-omics toolkits with traditional absolute measurements unlocks the scaling of core biological questions to dynamic and complex microbiomes, creating a deeper insight into inter-organismal relationships that drive the greater community function. (Bareche et al., 2018) used copy-number aberrations, somatic mutations and gene expression data to demonstrate the substantial genomic heterogeneity that characterizes TNBC molecular subtypes, allowing for a better understanding of the disease biology as well as the identification of several candidate targets paving novel approaches for the development of anticancer therapeutics for TNBC. (Singh et al., 2016) presented DIABLO (Data Integration Analysis for Biomarker discovery using a Latent component method for Omics studies) a multivariate analysis method based on the dimension reduction maximizing the correlation between each omics pairs. It underlines the importance of the processing of the interaction between omics data before using them for the prediction task.

Following this trend towards the integration of multi-omics data this work presents a machine learning algorithm based on pathways interactions between gene expression, epigenome expression and miRNAs expression to learn interpretable and sparse models uncovering potentially new candidate targets for the development of anticancer therapeutics for TNBC. The use of the multi-omics data helps emphasis the interaction between the different omics which leads to a better interpretation of the mechanism solution. Here we focus on the interpretable model because we strive to explain why these features are selected in the model decision path. There are two types of models in machine learning, generally speaking: the black box model and the interpretable model. An interpretable machine learning refers to methods and models that make the behaviour and predictions of machine learning systems understandable to humans. It differs from the black box model which is a system that does not reveal its internal mechanisms. Interpretability is more of a concept therefore there is no real mathematical definition of interpretability. A (non-mathematical) definition reported by (Miller, 2019) is: Interpretability is the degree to which a human can understand the cause of a decision. The need for interpretability here lies in the fact that for some tasks (especially the biological data), it is not enough to get the prediction (the what) (Doshi-Velez and Kim, 2017). The model must also explain how it came to the prediction (the why), because a correct prediction only partially solves your original problem (Molnar, 2019). Moreover, interpretability favours the acceptance of the model by health practitioners. Before the learning phase, there is a need to integrate the omics data. (Ritchie et al., 2015) define the integration of omics as the combination of multiple omics datasets to develop multivariate models to predict complex phenotypes. Mainly, it is the concatenation method (Liu et al., 2013) and the ensemble method (Günther et al., 2012). The concatenation method consists of putting all the omics together i.e. side-by-side and treating them as only one mega-set. The ensemble method consists of learning a classifier on each omics dataset and building a majority vote with the classifiers, for the final prediction. With time, new methods were also explored including the clustering (Rappoport et al., 2020) and the graph network ((Singh et al., 2016), (Heuschkel et al., 2020)). Here, in this work, the goal is to let the algorithm infer potential interaction between the features with the integration of new priors based on pathways of gene interactions. Therefore the concatenation method which does not imply any priors on the feature is more suitable for the task at hand. Depending on what a feature refers to, pathway-based feature selection methods can be classified into three categories: *pathway-level selection*, *bi-level selection* and *pathway-guided gene selection* (Tian et al., 2019). In the *pathway-level selection*, the goal is to select the whole pathways associated with the phenotypes of interest ((Dinu et al., 2007), (Wu et al., 2010)). The *bi-level selection* is a process, which identifies not only relevant pathways but also important genes that contribute critically to the significance of identified relevant pathways. In the *pathway-guided gene selection*, a feature corresponds to an individual gene.

The algorithm (GroupSCM) presented here is an extension of the Set Covering Machine (SCM) which was originally introduced by (Marchand and Shawe-Taylor, 2002). The SCM is a learning algorithm using a greedy approach to learn a conjunction set or a disjunction set of rules. The rules are the decision stumps (*omic_value_expression* $\leq v$ or *omic_value_expression* $\geq v$). The SCM applicability to the biomarker discovery task world is an effective algorithm in the domain. Kover (Drouin et al., 2016), a software used in the prediction of antibiotic resistance in bacteria is based on the SCM. This a robust algorithm yields great results in the antibiotic resistance prediction problem in accordance with the published literature. The *GroupSCM* extends the classical *SCM* to integrate the knowledge of variables interacting in biological pathways. The intuition behind this is to favour a rule selection based on their pathways association. The GroupSCM use the *pathway-guided gene selection* as priors and modify the utility function of the SCM into taking in account different weights on each feature depending on the pathways to which they belong.

2 METHODS

Let's $\mathcal{S}$ be a set of data such as $\mathcal{S} \stackrel{\text{def}}{=} \{(\mathbf{x}_i, y_i)\}_{i=0}^{m} \sim \mathcal{D}^m$ where $\mathbf{x}_i \in \mathcal{X}$ is a training example, $y_i \in \mathcal{Y}$ its associated label, $\mathcal{D}$ is a data generating distribution and m the size of the dataset. In this work, we consider the diagnosis of TNBC for a patient as a binary classification task where $\mathbf{x}_i$ represents the ith patient data (multi-omics features) and $y_i \in \{-1, 1\}$ whether the patient is TNBC or non-TNBC. Below we first describe the original SCM algorithm then we present our extension, the GroupSCM.

2.1 SCM

The SCM is an iterative algorithm whose goal is to produce either a conjunction of rules type model or a disjunction of rules type. It does so, by selecting the *rule* i with the maximum utility function at each iteration until there is no more examples or the number of rules predefined is reached. This is a maximization optimization algorithm type. At each iteration, a utility score U_i is computed for each of the remaining rules. Then an optimal *rule* i is selected ($i^* \leftarrow \underset{i}{\text{argmax}}\ U_i$) and so on to build a conjunction or disjunction of rules as the final model. Algorithm 1 presents the pseudo-code of the SCM. The SCM takes as input a set of examples (the training set) $\mathcal{S}$; the type of machine T which can be either a conjunction or a disjunction; a trade-off parameter p which influence how much we want to penalize the error on the positive examples and finally a parameter s which is the maximum number of rules to consider in the final results.

2.2 GroupSCM

The GroupSCM is based on the roots of the SCM. The goal of the GroupSCM is to overweight by a previously computed term, every utility score U_i of rules i belonging to the same pathway(s) as the selected rule(s) at the previous iteration. This overweight term is denoted the *prior of rule i* p_{ri}. All of the p_{ri} belong to the set $PR = \{p_{ri}\}_{i \in [1,n]}$ with n the number of features. In addition to the SCM inputs i.e $\mathcal{S}$, T, p and s, the GroupSCM also takes as an input PR and GR, the set of the groups for each rule already chosen. At the beginning i.e iteration 0, no rule is chosen therefore $GR = \emptyset$. Let's denote G the set of groups (pathway) $G = \{g_k\}$ with $k \in [1, |G|]$. PG is the set of the prior (preference) on the groups: $PG = \{p_g\}_{g \in [1,G]}$. For each rule ri, the corresponding rule prior p_{ri} is correlated to the sum of p_g: $p_{ri} = \exp(c \cdot (\sum_{g \in g_i} p_g))$. The priors of the rules p_{ri} are heavily dependent on the priors on the groups p_g. Therefore, p_g is where researchers and domain users should put their knowledge. Here we use a function that depends on the length of g_i. $p_g = f(-c \cdot |g|)$ with f: $f(x) = \exp(-c \cdot x)$. Algorithm 2 presents the pseudo-code.

2.3 Pathways Building

The pathways are retrieved from two (2) databases: BioGRID database (Stark et al., 2006) and MSigDB (Liberzon et al., 2011). BioGRID is an open-access database dedicated to the annotation and archival of protein, genetic and chemical interactions for all major model organism species including humans. The Molecular Signatures Database (MSigDB) is a collection of annotated gene sets for use with GSEA software. *78384* pathways of gene interactions are retrieved from BioGRID. In MSigDB, the targets are the gene sets that were curated from pathway databases. Usually, those genes sets are canonical representations of a biological process compiled by domain experts. There are *2232* canonical gene sets in MSigDB. MSigDB also provides great information on the miRNA. The miRNA gene sets extracted from MSigDB represent potential targets of regulation by transcription factors or microRNAs. The *1756* sets consist of genes grouped by elements they share in their non-protein-coding regions. In total there are *82372* gene sets (or pathways).

3 RESULTS

3.1 Datasets

The datasets were obtained from TCGA and all ethical regulations were followed. The samples used are those coming from the primary solid tumor (sample type code 01) and to the first vial (vial code A). The database contains numerous biological data types including DNA methylation, mRNA expression, miRNA expression, SNPs, and clinical information. The clinical view contains information regarding cancer stage, menopause status, race, and tumor status among others. The TNBC phenotype is retrieved from that clinical file by verifying the PR, ER, and HER2 phenotype i.e. positive or negative status. All the patients with negative PR, negative ER, and negative HER2 phenotypes are classified as TNBC patients and all the other combinations are classified as non-TNBC. There are 146 TNBC patients vs. 756 non-TNBC patients. It is worth noting that the dataset is a bit imbalanced (1 for 5).

The epigenome data is obtained using Illumina Methylation Assay technologies. There are 2 types of Illumina Methylation technologies: the 27k probes and the 450k probe technologies. Since TCGA is a collection of datasets from multiple independent studies, there are many discrepancies in the global dataset. For example, the information about the epigenome for some patients is either only available in the 27k technology or in the 450k technology and is sometimes altogether missing. In regards to this situation, we build a view denoted the methyl fusion view. It essentially consists of taking into account just the CpG available in both of the technologies (27k or 450k) to build a methyl fusion view for most of the patients. The new feature size of this methyl fusion view is 19984 CpG dinucleotides. The RNA expression data is available in 2 forms: the gene expressions (20531 features) and the genes isoforms expression, which includes splice variants, expressions (73599 features). The miRNA expression has 1046 features. Since the dimension is enormous, a variable selection based on the median absolute deviation (MAD) as presented in (Singh et al., 2016) was made. Two thousand (2000) features were selected from the methyl fusion view. The same amount was also selected from the RNA expression view and finally, two hundred and fifty (250) from the miRNAs view. The final dataset has 4250 features of CpGs, RNA, and miRNA. Each of the remaining CpGs sites and the RNA isoforms were linked to their corresponding genes names. When it is impossible to link the names of the gene to the features, the feature is discarded from the dataset. Once the dataset is finalized, the next logical step is the integration of the groups pathways. After that preprocessing, each feature is assigned to its corresponding pathways groups. If the feature does not belong to any pathways, it is classified into a new pathway created just for those types of features. For the GroupSCM experiments, two (2) variants of the dataset are used: one with all the features (902, 4250) and another without the features not belonging to a pathway (902, 4110).

3.2 Metrics

In this section, we present the different metrics used to evaluate the models learned. Since the problem is a classification task, four (4) metrics are reported: the Accuracy $\frac{tp+tn}{tp+fp+tn+fn}$, the F1 score $2 \cdot \frac{precision \cdot recall}{precision+recall}$, the Recall $\frac{tp}{tp+fn}$ and the Precision $\frac{tp}{tp+fp}$. tp stands for true positive; fp for false positive; tn for true negative and fn for false negative. Due to the data imbalance, the most important metric to look for to assess the performance of the models learned is the: F1 score. Being a mean between the precision and the recall, it is well suited to understand the model performance on both the positive and negative examples simultaneously.

3.3 Experiments Results

All the experiments and their results are presented here. Initially, two algorithms are evaluated: the Decision Trees (DT) and the Set Covering Machine (SCM) on the dataset. These evaluations serve as the baseline results to compare the results of the GroupSCM experimentation. As stated before, the multi-omics data combination used here is *CpG - RNA isoforms - miRNA*. To eliminate the randomness due to the creation of the train - test splits, the experiments are run *15* times with different random train - test splits at different random seeds. The dataset is split using the 80/20 % split i.e. 80% for the training set and 20% for the test set. In the learning phase, a 5-fold cross-validation is applied to select the best hyperparameters. If not stated otherwise the metrics score presented here are only the metrics on the test set.

At each run, i.e. for each split the metrics on the test and train sets are reported and an average is computed to see the mean performance of the algorithms overall. Figure 2 shows the main results of

Algorithm 1: Set Covering Machine.

```
procedure SCM(S, p, s, T, $\mathcal{R}$)
    $INPUT$ : S: A set of m training examples, T: a type of machine conjunction or disjunction, p: The class trade-of parameter, s: The maximum number of rules in h, $\mathcal{R} = \{r_i(\mathbf{x})\}^{|\mathcal{R}|_{i=1}}$: a set of boolean-valued rules;
    $\mathcal{R}^* \leftarrow \phi$
    $\mathcal{P} \leftarrow$ the set of examples in $\mathcal{S}$ with label 1
    $\mathcal{N} \leftarrow$ the set of examples in $\mathcal{S}$ with label 0
    stop ← False
    while $\mathcal{N} \neq \phi$ or $|\mathcal{R}^*| \leq s$ or $\neg$stop do
        $\forall r_i in \mathcal{R}$, $N_i \leftarrow$ the subset of N correctly classified by $r_i$
        $\forall r_i in \mathcal{R}$, $\overline{P}_i \leftarrow$ the subset of P correctly misclassified by $r_i$
        $\forall r_i in \mathcal{R}$, $U_i = |N_i| - p \cdot |\overline{P}_i|$ if $|N_i| \geq |\overline{P}_i|$ and $-\infty$ otherwise
        $i^* \leftarrow \underset{i}{\text{argmax}}\, U_i$
        if $U_{i^*} \neq \infty$ then and $|N_{i^*}| > 0$ or $|\overline{P}_{i^*}| > 0$
            $\mathcal{R}^* \leftarrow \mathcal{R}^* \cup r_{i^*}$
            $\mathcal{N} \leftarrow \mathcal{N} - N_{i^*}$
            $\mathcal{P} \leftarrow \mathcal{P} - \overline{P}_{i^*}$
        else
            stop = True
    return h, where $h(x) = \bigwedge_{r_i^* \in \mathcal{R}^*} r_i^*(\mathbf{x})$ if T = conjunction or $h(x) = \bigvee_{r_i^* \in \mathcal{R}^*} r_i^*(\mathbf{x})$ if T = disjunction
```

Algorithm 2: Group Set Covering Machine (GroupSCM) (in bold the principal differences between SCM and GroupSCM.

```
 1: procedure GROUPSCM(S, T, p, s, PR,GR, $\mathcal{R}$)
 2:     $INPUT$ : S: A set of training examples, T: a type of machine conjunction or disjunction, p: The class trade-of parameter, s: The maximum number of rules in h, $\mathbf{PR} = \{\mathbf{p_{ri}}\}_{\mathbf{i \in [1,n]}}$, $\mathcal{R} = \{r_i(\mathbf{x})\}^{|\mathcal{R}|_{i=1}}$: the set of boolean rules; GR the subset of the groups chosen
 3:     $OUTPUT$ : A conjunction or a disjunction f(x) of a subset $\mathbb{R} \subseteq \mathcal{H}$
 4:     $\mathcal{R}^* \leftarrow \phi$
 5:     $\mathcal{P} \leftarrow$ the set of examples in $\mathcal{S}$ with label 1
 6:     $\mathcal{N} \leftarrow$ the set of examples in $\mathcal{S}$ with label 0
 7:     stop ← False
 8:     while $\mathcal{N} \neq \phi$ or $|\mathcal{R}| \leq s$ or $\neg$stop do
 9:         $\forall r_i in \mathcal{R}$, $N_i \leftarrow$ the subset of N correctly classified by $r_i$
10:         $\forall r_i in \mathcal{R}$, $\overline{P}_i \leftarrow$ the subset of P correctly misclassified by $r_i$
11:         $\forall r_i in \mathcal{R}$, $\mathbf{U_i} = \big[|\mathbf{N_i}| - \mathbf{p} \cdot |\overline{\mathbf{P}}_\mathbf{i}|\big] \cdot \mathbf{p_{ri}}$ if $|N_i| \geq |\overline{P}_i|$ and $-\infty$ otherwise
12:         $i^* \leftarrow \underset{i}{\text{argmax}}\, U_i$
13:         Tie break choose $\mathbf{i}^*$ such as $\underset{|\mathbf{g_i^*}|}{\text{argmin}}$
14:         Update PR: For all remaining rules,
15:             ▷ Case 1: favor rules from same group (inner group) $\mathbf{p_{ri}} = \mathbf{p_{ri}} * \exp(|\mathbf{g_i} \cup \mathbf{GR}|)$
16:             ▷ Case 2: favor rules from different groups (outer group) $\mathbf{p_{ri}} = \mathbf{p_{ri}} * \exp(-|\mathbf{g_i GR}|)$
17:         Update GR $\leftarrow \mathbf{GR} \cup \mathbf{g_k}$ with $\mathbf{g_k}$ the groups/pathways of rules choosen at 12
18:         if $U_{i^*} \neq \infty$ then and $|N_{i^*}| > 0$ or $|\overline{P}_{i^*}| > 0$
19:             $\mathcal{R}^* \leftarrow \mathcal{R}^* \cup r_{i^*}$
20:             $\mathcal{N} \leftarrow \mathcal{N} - N_{i^*}$
21:             $\mathcal{P} \leftarrow \mathcal{P} - \overline{P}_{i^*}$
22:         else
23:             stop = True
24:     return h, where $h(x) = \bigwedge_{r_i^* \in \mathcal{R}^*} r_i^*(\mathbf{x})$ if T = conjunction or $h(x) = \bigvee_{r_i^* \in \mathcal{R}^*} r_i^*(\mathbf{x})$ if T = disjunction
```

Table 1: Mean F1 Scores from the best seed for each algorithm and the best values from the best seed. * is the GroupSCM applied to the dataset without the features without a pathway. c is the value of the hyperparameter of the GroupSCM.

Algorithm	Mean Metrics Values		Best Metrics Values	
DT	0.89 +/- 0.03		0.94	
SCM	0.91 +/- 0.03		0.96	
GroupSCM	*Outer*	*Inner*	*Outer*	*Inner*
	c=0.4; 0.88 +/- 0.04	c=0.1; 0.88 +/- 0.04	0.94	0.96
GroupSCM*	c=0.1; 0.83 +/- 0.07	c=0.1; 0.83 +/- 0.07	0.90	0.90

the experiments. The F1-Score with the DT models is: *0.89 +/- 0.03* (fig 2 a). The F1-Score with the SCM models is : *0.91 +/- 0.03* (fig 2 b). The baseline scores can be judged as good scores since they are around 90%. The SCM slightly outperforms the DT. The models decision paths are similar between the SCM and the DT. Indeed on the 15 repetitions, the DT outputs exclusively uc002vwt.2_MLPH as the only tree 4 times and uc002vwt.2_MLPH as the root of the trees 9 other times. Meanwhile, the SCM outputs uc002vwt.2_MLPH as the only rule 9 times and in a conjunction of rules 3 other times. Figure 1 presents the number of features retrieve by each algorithm at each of the 15 seeds. The SCM is mostly the sparser model at each seed followed by the GroupSCM extension then the DT. Furthermore, to better investigate the biomarkers retrieved, only the biomarkers selected by the model with the best F1 score on the test set will be analyzed. The best model obtains by the DT is a tree with only root uc002vwt.2_MLPH with *0.94* F1 score. The best model obtains by the SCM is a conjunction of rules uc002vwt.2_MLPH, uc002hul.3_RARA, uc009wsd.2_HDGF and uc001jpo.1_TSPAN15 with *0.96* F1 score.

The last two plots in the Figure 2 show the results of the GroupSCM on the dataset with all the features (fig 2 c) and the dataset without the features not belonging to a pathway (fig 2 d). With all the same features (fig 2 c), GroupSCM performs relatively like the SCM metrics-wise. Indeed with the best hyperparameters, the average F1 score is *0.88 +/- 0.04*. The best model has an F1 score of *0.96*. Meanwhile, the rules chosen are totally different from the ones obtained from the baseline results. The rules selected here are a conjunction of cg17095936_TBX19, cg10305797_KRTDAP, and cg18267381_ZNF385D. Their respective belonging pathways are: [G_82372], [G_82372], [G_82372]. This is the same pathway. The immediate conclusion from this is the effectiveness of the prior given the fact that it helped guide the decision paths of the algorithm. However, G_82372 is the pathway of the features that did not belong to any pathway within the databases data. Therefore even though this is a great result there is a lack of biological interpretation with this result. Why? Because the biological impact of the pathways cannot be explained directly here.

The final experimentation explores the performance of the GroupSCM on the dataset without the features that did not belong to any pathway within the databases data retrieved. This experiment is more suitable to correctly assess the performance of the prior and the algorithm overall. With the best hyperparameters, the average F1 score is *0.82 +/- 0.05* on the test set (fig 2 d). Despite being roughly 9% lower than the simple SCM and the GroupSCM on the complete dataset, this is still a good score since it's over 80% on average. The best model from this experimentation has *0.90* F1 score. This model selects the conjunction of these rules: hsa-mir-18a and hsa-mir-190b. Table 1 presents a summary of all the results of all the experimentation. One important observation to notice is the fact that the score values are not different from the inner-group our outer-group update (see algorithm 2). Another important observation is despite the drop in performance, the algorithm is still pretty good but is also more sparse on the pathways levels. Most of the new rules selected belong to one pathway. Therefore their interaction can be biologically interpreted and analyzed. In table 2 the features selected by the best model for each experiment are presented. Along with those features, the pathways to which they belong are also presented.

4 DISCUSSION

In this paper, we tackle the breast cancer triple negative prediction problem with the purpose of providing an interpretable and sparse model. We elect to do this task by learning a GroupSCM which is essentially a SCM with a prior on the rules selection. The new utility function is set to increase the weights of the rules previously selected in the previous iteration. There are two types of overweighting process used in the algorithm: the inner-group-weighting and the outer-group-weighting. In the first case (the inner-

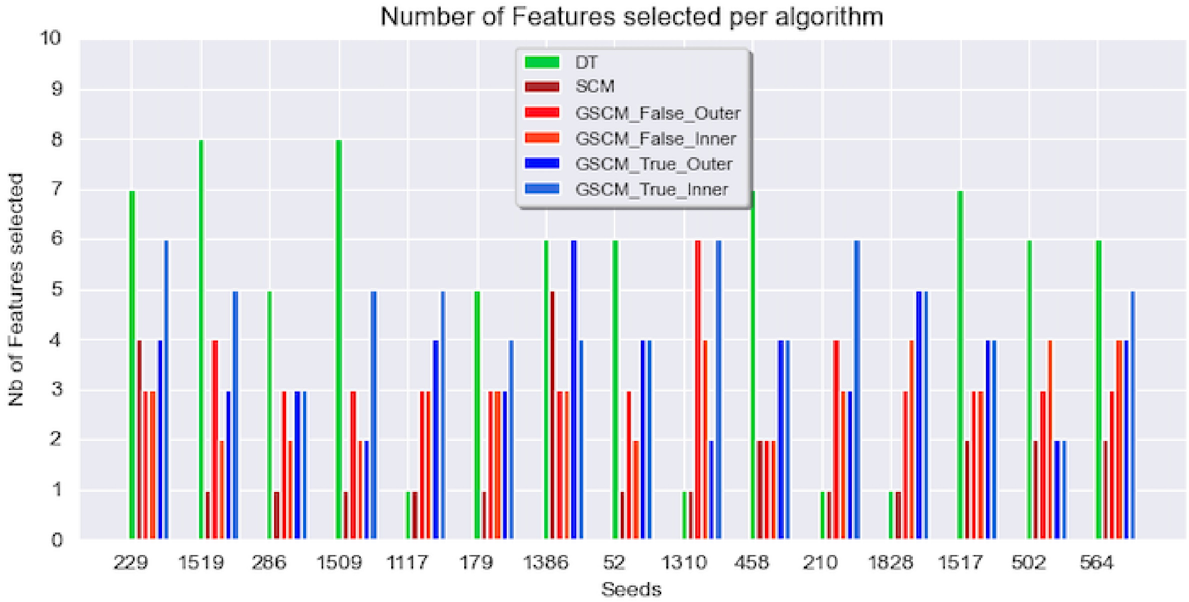

Figure 1: Number of feature return per algorithm at each seed (iteration).

Table 2: Features and Pathways selected by the best model of each algorithm type.

Algorithm	Features	Pathways
DT	uc002vwt.2_MLPH	[G_455, G_1029, G_10245, G_11700, G_15952, G_25302, G_30827, G_33710, G_44607, G_51709, G_52337]
SCM	uc002vwt.2_MLPH, uc002hul.3_RARA, uc009wsd.2_HDGF, uc001jpo.1_TSPAN15	Not Shown (too much values)
GroupSCM	cg17095936_TBX19, cg10305797_KRTDAP, cg18267381_ZNF385D	[G_82372], [G_82372], [G_82372]
GroupSCM*	hsa-mir-18a, hsa-mir-190b	[G_80747], [G_81521]

group case), if the model selects some rules outside the same pathways the conclusion is that the correct explanation (from the experiment) is *inter-groups* related (since the rules belong to different pathways). In the second case (the outer-group case), if the model selects rules from the same pathways (i.e. it uses the priors) meaning that the correct explanation is *intra-groups* related. But overall, looking at the results in table 1, the metric scores are not different from inner versus outer update for the GroupSCM. Even if it is for different c values. Despite being a little bit less performing than the SCM, the GroupSCM produce sparser rules: three rules selected versus five rules selected for the SCM. This comparison is on the dataset with all the features. The results are even sparser when considering the experiment with just the features belonging to a known pathway. This situation selects two rules. The sparser model implies easier *in vivo* experimentation and validation.

Interestingly, the SCM selects almost all rules in the RNA omics components and the GroupSCM select the rules either in the CpGs omics part or the miRNA part (table 2). The main observation here is while both the DT and the SCM seem to select only RNA isoforms rules therefore the RNA omics views only, the GroupSCM overlooks this view to select rules from either the CpGs (methylome view) or the miRNA (miRNA views). This is useful finding since CpGs and miRNA impact the translation therefore the gene expressions levels. Biologically speaking, the algorithm is putting greater emphasis on the upstream of the biology principal theory. Let's recall here one of the hidden goals is to see how well investigating all the omics together would perform on the prediction task of determining the TNBC vs. non-TNBC patients. In that case, the algorithm still concentrates on just one component of the omics view but in a more integrative fashion. Indeed knowing if the CpGs sites are hyper or under methylated is also informative on the genes expression level, since we have the pathways of the genes, those sites regulate. It is a similar process for the miRNA. Their levels of expression (over or under) also affect the gene expressions level, and knowing their pathways, we can see the downstream impact of the miRNAs on gene expressions. The GroupSCM enables a bigger picture

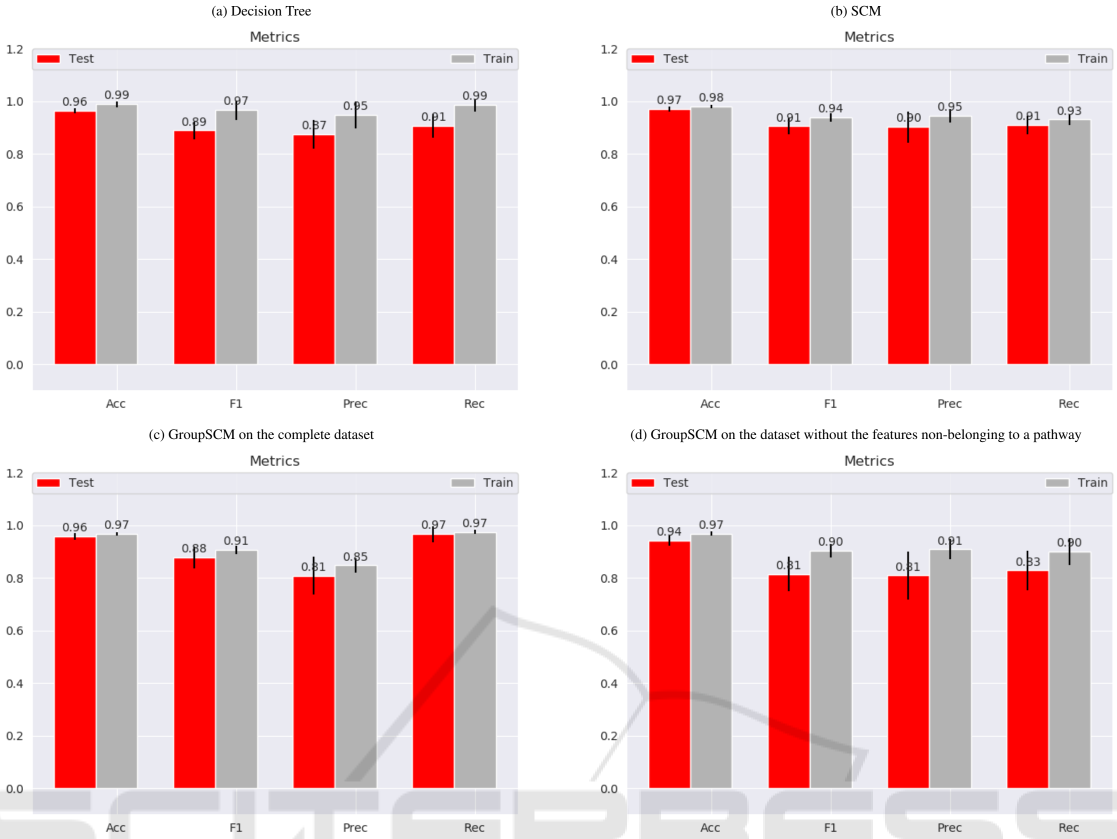
(a) Decision Tree

(b) SCM

(c) GroupSCM on the complete dataset

(d) GroupSCM on the dataset without the features non-belonging to a pathway

Figure 2: DT-SCM-GroupSCM Mean Metrics Results (Accuracy, F1-score, Precision and Recall)(Train (Gray) Test (Red)).

and observation of the biomarker discovery process in a more global way.

We elect to analyze the features returned by the GroupSCM in the experiment without the features not belonging to a pathway. The model obtains from this experimentation is a two-rule conjunction: hsa-mir-18a and hsa-mir-190b. According to (Weizmann, 2020a) diseases associated with mir18A include thyroid gland anaplastic carcinoma and medulloblastoma. Among its related pathways are Parkinson's disease pathway and DNA damage response. In our database: mir18A belongs to pathway G_80747 in our experimentation (http://mirdb.org/cgi-bin/mature_mir.cgi?name=hsa-miR-18a-3p). This biomarker is known to heavily impact numerous pathways or interactions in many cancers. (Komatsu et al., 2014) described mir18A as an important biomarker in cancer since mir18A, which is located in the potentially oncogenic miR-17-92 cluster, is a highly expressed microRNAs in several types of cancers. (Li et al., 2016) demonstrated that tamoxifen resistance in breast cancer cells is enhanced through a miR-18a-HIF1 feedback regulatory loop. Recently, (Zhang et al., 2019) also showed that SREBP1, targeted by miR-18a-5p, modulates epithelial-mesenchymal transition in breast cancer via forming a co-repressor complex with Snail and HDAC1/2. This literature review confirms that our algorithm targets an already known biomarker in cancer studies. But there is no link specifically to the TNBC phenotype. According to (Weizmann, 2020b), there are no diseases linked to mir190B. Nevertheless, (Cizeron-Clairac et al., 2015) proved that mir190B is the highest up-regulated miRNA in ER-positive compared to ER-negative breast tumors. Making it a potential new biomarker for the triple-negative breast cancer. (Zhao et al., 2020) recently demonstrated that long non-coding RNA TUSC8 inhibits breast cancer growth and metastasis via miR190b-5p/MYLIP axis. These evidences show the ability of our model to discover biomarkers for the TNBC prediction problem. As we can see for both of these miRNAs there is no direct connection between them and the TNBC phenotype but our study suggests otherwise. The next step will be to analyze those biomarkers in *in vivo* settings to have solid confirmation of the discovery. We proceeded with a statistical analysis of the biomarkers retrieved and analyzed the expression level in the population with the classical t-test and the p-values. In figure 3 we plotted the expression levels of both

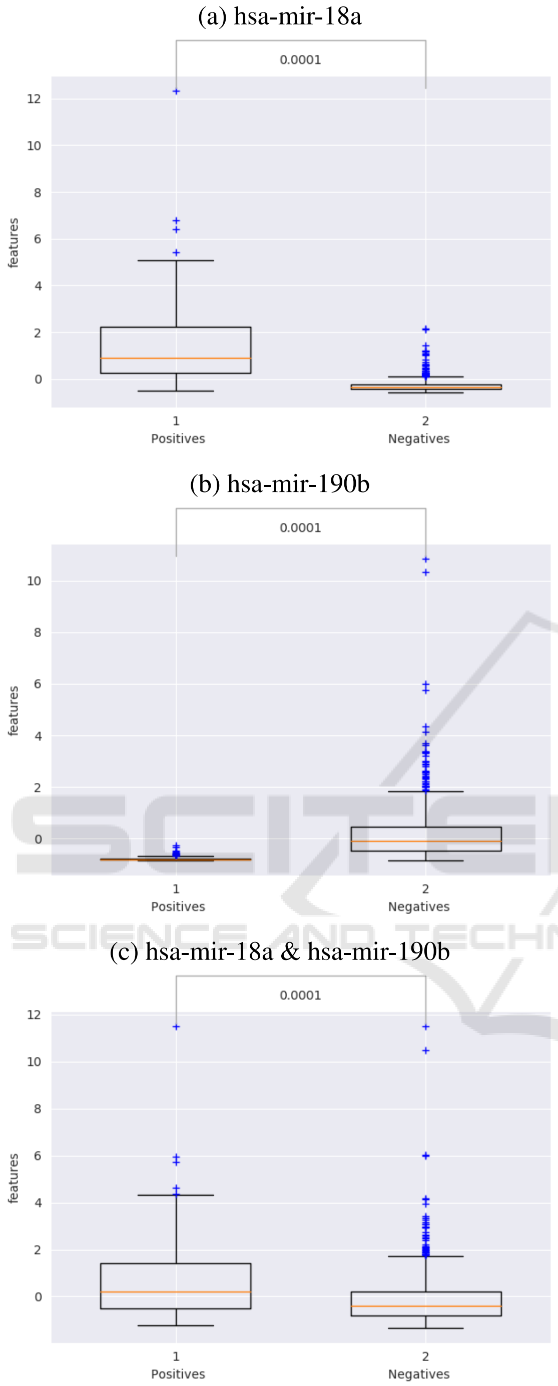

(a) hsa-mir-18a

(b) hsa-mir-190b

(c) hsa-mir-18a & hsa-mir-190b

Figure 3: Expression levels of the hsa-mir-18a (a), hsa-mir-190b (b) and both (c) in the TNBC vs non-TNBC.

features independently alone (fig 3 a & b) and together. The conclusion is both of them are statistically significant with hsa-mir-18a more expressed in the TNBC and hsa-mir-190b in the non-TNBC. Together they are substantially expressed in the TNBC examples improving the significance.

5 CONCLUSION

We present and apply an extension of the SCM to an algorithm using a prior on the pathways of appartenance of the features. In this particular case, the algorithm yields interesting results biomarkers while maintaining a good statistical scores overall. This algorithm is a good addition to the precision medicine field using the pathway interaction to find the appropriate biomarkers related to a specific disease. It is sparse and interpretable which suits clinician expectations. Despite the findings, additional *in vivo* experimentations should be completed continuing the improvements of the model performance of data-driven predictions and to provide validated evidence linking specific biomarkers to a disease phenotype.

COMPETING INTERESTS

The authors declare that they have no competing interests.

AUTHOR'S CONTRIBUTIONS

OMA designed the algorithm and the experimentation and wrote this article. PT co-designed the algorithm. JC and FL supervised the work and contributed to the redaction of the manuscript.

ACKNOWLEDGEMENTS

A special thanks to Emmanuel Noutahi for his inputs in this work. The work was supported by the Canada Research Chair in Medical genomics (JC), Compute Canada, Institute Intelligence and Data (IID) and Centre de recherche en données massives (CRDM).

REFERENCES

Bareche, Y., Venet, D., Ignatiadis, M., Aftimos, P., Piccart, M., Rothe, F., and Sotiriou, C. (2018). Unravelling triple-negative breast cancer molecular heterogeneity using an integrative multiomic analysis. *Annals of Oncology*, 29(4):895–902.

Cizeron-Clairac, G., Lallemand, F., Vacher, S., Lidereau, R., Bieche, I., and Callens, C. (2015). Mir-190b, the highest up-regulated mirna in erα-positive compared to erα-negative breast tumors, a new biomarker in breast cancers? *BMC cancer*, 15(1):499.

Delogu, F., Kunath, B., Evans, P., Arntzen, M., Hvidsten, T., and Pope, P. (2020). Integration of absolute multi-omics reveals dynamic protein-to-rna ratios and metabolic interplay within mixed-domain microbiomes. *Nature Communications*, 11(1):1–12.

Dinu, I., Potter, J. D., Mueller, T., Liu, Q., Adewale, A. J., Jhangri, G. S., Einecke, G., Famulski, K. S., Halloran, P., and Yasui, Y. (2007). Improving gene set analysis of microarray data by sam-gs. *BMC bioinformatics*, 8(1):242.

Doshi-Velez, F. and Kim, B. (2017). Towards a rigorous science of interpretable machine learning. *arXiv preprint arXiv:1702.08608*.

Drouin, A., Giguère, S., Déraspe, M., Marchand, M., Tyers, M., Loo, V. G., Bourgault, A.-M., Laviolette, F., and Corbeil, J. (2016). Predictive computational phenotyping and biomarker discovery using reference-free genome comparisons. *BMC genomics*, 17(1):1–15.

Freedman, M. L., Monteiro, A. N., Gayther, S. A., Coetzee, G. A., Risch, A., Plass, C., Casey, G., De Biasi, M., Carlson, C., Duggan, D., et al. (2011). Principles for the post-gwas functional characterization of cancer risk loci. *Nature genetics*, 43(6):513–518.

Günther, O. P., Chen, V., Freue, G. C., Balshaw, R. F., Tebbutt, S. J., Hollander, Z., Takhar, M., McMaster, W. R., McManus, B. M., Keown, P. A., et al. (2012). A computational pipeline for the development of multi-marker bio-signature panels and ensemble classifiers. *BMC bioinformatics*, 13(1):326.

Heuschkel, M. A., Skenteris, N. T., Hutcheson, J. D., van der Valk, D. D., Bremer, J., Goody, P., Hjortnaes, J., Jansen, F., Bouten, C. V., van den Bogaerdt, A., et al. (2020). Integrative multi-omics analysis in calcific aortic valve disease reveals a link to the formation of amyloid-like deposits. *Cells*, 9(10):2164.

Iorio, M. V., Ferracin, M., Liu, C.-G., Veronese, A., Spizzo, R., Sabbioni, S., Magri, E., Pedriali, M., Fabbri, M., Campiglio, M., et al. (2005). Microrna gene expression deregulation in human breast cancer. *Cancer research*, 65(16):7065–7070.

Karczewski, K. J. and Snyder, M. P. (2018). Integrative omics for health and disease. *Nature Reviews Genetics*, 19(5):299.

Komatsu, S., Ichikawa, D., Takeshita, H., Morimura, R., Hirajima, S., Tsujiura, M., Kawaguchi, T., Miyamae, M., Nagata, H., Konishi, H., et al. (2014). Circulating mir-18a: a sensitive cancer screening biomarker in human cancer. *in vivo*, 28(3):293–297.

Lao, V. V. and Grady, W. M. (2011). Epigenetics and colorectal cancer. *Nature reviews Gastroenterology & hepatology*, 8(12):686.

Lehmann, B. D., Bauer, J. A., Chen, X., Sanders, M. E., Chakravarthy, A. B., Shyr, Y., and Pietenpol, J. A. (2011). Identification of human triple-negative breast cancer subtypes and preclinical models for selection of targeted therapies. *The Journal of clinical investigation*, 121(7):2750–2767.

Li, X., Wu, Y., Liu, A., and Tang, X. (2016). Long non-coding rna uca1 enhances tamoxifen resistance in breast cancer cells through a mir-18a-hif1α feedback regulatory loop. *Tumor Biology*, 37(11):14733–14743.

Liberzon, A., Subramanian, A., Pinchback, R., Thorvaldsdóttir, H., Tamayo, P., and Mesirov, J. P. (2011). Molecular signatures database (msigdb) 3.0. *Bioinformatics*, 27(12):1739–1740.

Liu, Y., Devescovi, V., Chen, S., and Nardini, C. (2013). Multilevel omic data integration in cancer cell lines: advanced annotation and emergent properties. *BMC systems biology*, 7(1):14.

Marchand, M. and Shawe-Taylor, J. (2002). The set covering machine. *Journal of Machine Learning Research*, 3(Dec):723–746.

Miller, T. (2019). Explanation in artificial intelligence: Insights from the social sciences. *Artificial Intelligence*, 267:1–38.

Molnar, C. (2019). *Interpretable Machine Learning*. https://christophm.github.io/interpretable-ml-book/.

Rappoport, N., Safra, R., and Shamir, R. (2020). Monet: Multi-omic module discovery by omic selection. *PLOS Computational Biology*, 16(9):e1008182.

Ritchie, M. D., Holzinger, E. R., Li, R., Pendergrass, S. A., and Kim, D. (2015). Methods of integrating data to uncover genotype-phenotype interactions. *Nature reviews. Genetics*, 16(2):85.

Singh, A., Gautier, B., Shannon, C. P., Vacher, M., Rohart, F., Tebutt, S. J., and Le Cao, K.-A. (2016). Diablo-an integrative, multi-omics, multivariate method for multi-group classification. *bioRxiv*, page 067611.

Stark, C., Breitkreutz, B.-J., Reguly, T., Boucher, L., Breitkreutz, A., and Tyers, M. (2006). Biogrid: a general repository for interaction datasets. *Nucleic acids research*, 34(suppl_1):D535–D539.

Tian, S., Wang, C., and Wang, B. (2019). Incorporating pathway information into feature selection towards better performed gene signatures. *BioMed research international*, 2019.

Weigelt, B., Baehner, F. L., and Reis-Filho, J. S. (2010). The contribution of gene expression profiling to breast cancer classification, prognostication and prediction: a retrospective of the last decade. *The Journal of Pathology: A Journal of the Pathological Society of Great Britain and Ireland*, 220(2):263–280.

Weizmann, I. o. S. (2020a). Mir18a. https://www.genecards.org/cgi-bin/carddisp.pl?gene=MIR18A. Accessed: 2020-10-21.

Weizmann, I. o. S. (2020b). Mir190b. https://www.genecards.org/cgi-bin/carddisp.pl?gene=MIR190B. Accessed: 2020-10-21.

Wu, D., Lim, E., Vaillant, F., Asselin-Labat, M.-L., Visvader, J. E., and Smyth, G. K. (2010). Roast: rotation gene set tests for complex microarray experiments. *Bioinformatics*, 26(17):2176–2182.

Yuan, Y., Liu, L., Chen, H., Wang, Y., Xu, Y., Mao, H., Li, J., Mills, G. B., Shu, Y., Li, L., et al. (2016). Comprehensive characterization of molecular differences in cancer between male and female patients. *Cancer cell*, 29(5):711–722.

Zhang, N., Zhang, H., Liu, Y., Su, P., Zhang, J., Wang, X., Sun, M., Chen, B., Zhao, W., Wang, L., et al. (2019).

Srebp1, targeted by mir-18a-5p, modulates epithelial-mesenchymal transition in breast cancer via forming a co-repressor complex with snail and hdac1/2. *Cell Death & Differentiation*, 26(5):843–859.

Zhao, L., Zhou, Y., Zhao, Y., Li, Q., Zhou, J., and Mao, Y. (2020). Long non-coding rna tusc8 inhibits breast cancer growth and metastasis via mir-190b-5p/mylip axis. *Aging (Albany NY)*, 12(3):2974.